Lidar studies of the cloud top height over ocean

I.E. Penner and V.S. Shamanaev

Institute of Atmospheric Optics, Siberian Branch of the Russian Academy of Sciences, Tomsk

Received June 15, 1999

To approbate the technique of laser sounding of clouds as the means of satellite underflight measurements, two experiments have been conducted from an aircraft flying over the Barents Sea along complex routes. The total length of the routes was about several hundred kilometers. Cloud fields were studied at the stages of their formation and dissipation. Power spectra of fluctuations of the cloud top height have been calculated. It is shown that they differ for different types of clouds.

In climate and weather studies, special attention is paid to the process of interaction of solar radiation with clouds. An inhomogeneous spatial structure of clouds plays an important part in these processes. Simplified representation of the stochastic geometry of the cloud top height can cause a significant bias in calculated results on the radiative processes.[1] Experimental information obtained at laser sounding of cloudiness from onboard an aircraft allows one to develop more realistic models of cloudiness. To facilitate the studies of that sort, a lidar is an indispensable instrument for obtaining experimental data on the cloud top height with high spatial resolution (several meters) for cloud fields with typical horizontal size from tens of meters to hundreds of kilometers. Longer sections can hardly be observed for purely aviation reasons. For several years we have conducted airborne experiments on laser sounding of atmospheric formations and the underlying surface over northern seas and the territory of the Western Siberia. In the course of these studies we have compiled a lot of data on the cloud top height of low-level clouds, which are most often stratocumulus. Based on these data, statistically confident analysis of the spatial structure of stratocumulus has been performed.

The cloud top was sounded by a Svetozar–3 and a Makrel polarization lidars[2] installed aboard an IL–14FKM and IL–18DORR instrumented airplanes. The sounding scheme was the same in all the cases. As an aircraft flew along a given route over a cloud field, the lidar sounded clouds by transmitting pulses at the wavelength of 532 nm downward through a hatch in the aircraft bottom. The lidar recording system either recorded full profiles of return signals backscattered at the wavelength of sounding radiation or measured the distance to the cloud top at some characteristic points using a preset algorithm. Absolute values of the cloud top height in the latter case were estimated as the difference between the flight altitude, which could be rather accurately determined by the aircraft navigation equipment, and the distance from the aircraft to a cloud measured with the lidar.

A laser pulse length, which determines the limiting spatial resolution in height for all types of lasers, was within 20 ns. The spatial resolution along the horizontal path was from 5 to 20 meters depending on the flight speed and the pulse repetition frequency. It was assumed that the flight speed was constant, and the spatial structure of cloud fields changed insignificantly during the experiment (it was from ten minutes to one hour). The latter assumption is based on the fact that the stages of evolution of the fields of *St-Sc* clouds take, on the average, far longer time (from tens of hours to several days).[3] These assumptions allow us to pass from the actual time-frequency representation of the measurement data to their expansion over spatial wave numbers $k_i = 2\pi/\lambda_i$, where λ_j are the spatial wavelengths of cloud motions.

Cloud physics equations show that the mean heights of the cloud top and base are related in some complex way, to the vertical temperature lapse rate, the altitude of tropopause, the turbulent exchange coefficient, and the specific gas constants of air and water vapor.[3] In the general case, height fluctuations result from the three processes: slow systematic changes associated with the change of the atmospheric field of humidity, changes due to air flows, and turbulent fluctuations.

However, there is no common treatment accepted for the terms “cloud topB and “cloud base,B since climatology, aviation, and aerosol physics employ different criteria. Lidar allows determination of the distance to a cloud by several (at least, five) criteria associated with different branches of practices. They are exemplified in Fig. 1 with the general profile of a lidar return signal $F(r)$ (Ref. 4). It is rather natural that they introduce a bias in the absolute value of the distance to a cloud, that depends on the structure of the cloud boundary. At the same time, relative changes in this distance determined according to these criteria, correlate quite well with the correlation coefficient close to unity (0.98). This statement was supported by the results of *in situ* experiments, in which the distance to the cloud top (upper cloud boundary) was determined by the beginning and the maximum of a return signal from a cloud and by the excess over a given threshold amplitude.[5] Therefore, in the further measurements a single criterion was used for certainty. This criterion was based on the excess of the signal amplitude over a

0235-6880/99/12 1093-05 $02.00

preset threshold value. The threshold was set as a sum of two terms: the level of the return signal from the pure atmosphere directly above the cloud and the doubled rms background value obtained at the tail of a return signal, i.e., actually at the infinity (in Fig. 1 this corresponds to a point somewhere far from the point r_0).

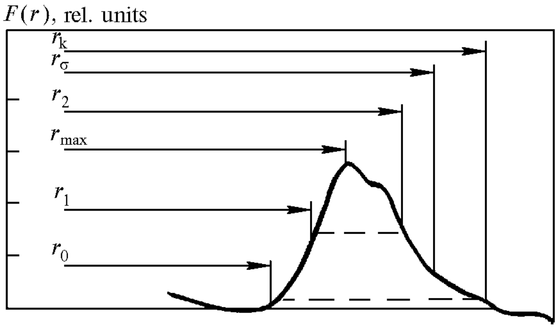

Fig. 1. Cloud boundary as determined with a lidar. $F(r)$ is the power of a lidar return signal from a cloud and the preceding layer of the atmosphere. At the point r_0 the signal from a cloud begins to excess the background signal from the atmosphere; r_1 is the threshold value of the signal at the leading edge of the return signal; r_{max} is the maximum value, at which the first derivative is zero; r_2 is the signal value at the trailing edge; r_σ is the depth into the cloud at which the extinction coefficient achieves a preset value, for example, $\sigma = 5$ km^{-1}. The point r_k indicates the final depth of cloud sounding at a certain threshold.

To avoid a complication of the pattern of cloud height fluctuations, we do not consider here the scattering coefficient.

In processing we used the data obtained at different time and over different geographic regions. Besides, in the case of broken cloud fields and abrupt changes in the height, discontinuities and gaps of the first kind arise in the arrays of data on the cloud top heights. Therefore, one of the main steps in preparation of these data for processing by statistical methods is formation of a continuous set of discrete values of the cloud height obtained in different cloud fields. Certainly, information on the most large-scale processes and absolute values of changes is lost in this case. However, since we are interested in estimates of statistical parameters of the cloud top spatial structure, it is reasonable to consider only fluctuations of the cloud top height, irrespective of its absolute value. Toward this end, we transform the initial samples of height values $\{H_n\}$ into a new set $\{h_n\}$, which has a zero sample-mean value:

$$\{h_n\} = h(t_0 + n\Delta t) = H_n - \langle H_n\rangle,\ n = 1, 2 \ldots N;$$

where n is the running number of a sounding pulse; t_0 is the time of beginning of the sounding; $\Delta t = 1/f_l$ is the period of sounding over the flight route; $\langle H\rangle$ is the sample-mean height in one realization, and N is a finite number of the height values in this realization. Here f_l is the laser pulse repetition frequency.

Besides, for each realization we made normalization to the rms deviation σ_h obtained from the variance σ_h^2 of the transformed sample h_n. Thus, the probability densities of height fluctuations for different cloud fields can be compared on the same scale of σ_h^2 values.

At the next stage, the sample-mean values $\langle H_n\rangle$ for all realizations were averaged once more over the cloud field for a particular day of sounding. The calculated average height H_0 of a specific cloud field is given in Table 1. (According to the morphological classification of clouds,[3] the values of these heights indicate that the cloud fields studied belonged to the same family of low-level clouds.)

Table 1. The initial data of sounding of the marine cloud top height with an airborne lidar

Date	Nov 27, 1987	Nov 29, 1987
Region	Barents Sea	
Cloud type	*St*	*Sc*
Cloud amount	10	8–9
Spatial resolution in height Δh, m	4	4
Spatial resolution along the route Δl, m	20	20
Average height H_0, m	1550	1800
Total route length L, km	500	380
Number of cloud top values, N	22000	18000

The initial data may contain trends or low-frequency components, whose assumed period is far longer than the period of a realization $\{H_n\}$. Combining individual realizations into a continuous set of values of the cloud top heights of a single cloud field in the presence of discontinuous trends can result in significant distortions of the estimates of the probability density and spectral characteristics in the subsequent analysis. Such trends were removed from limited, in size, realizations by approximating the initial data using a low-order polynomial. According to classical recommendations,[6] we mostly removed the linear trends.

The set of cloud top heights prepared in such a way is a random process of fluctuations of the cloud top height with a zero mean and unit variance. Low-frequency components that do not fit the actually measured spatial scale of the size of one realization were removed from this set either. The data were also smoothed to suppress the most high-frequency components, which are caused by artifacts arising under conditions of the low signal-to-noise ratio in the return signals. All such files were checked for the steadiness of the processes they represent. To do this, we have constructed empirical probability densities of the distribution of cloud top heights (more precisely, their deviations from the zero mean). They were approximated by Gaussian curves. Then the rms deviation of the calculated distributions from the model ones was calculated.

Table 1 gives the initial data of sounding cloudiness in several long flights. Here we do not consider flights over cumulus. The AN–30 aircraft used can fly only over *Cu med* (cumulus of fine weather) clouds. However, statistical analysis used in this paper cannot be applied to describe such a broken structure as the cumulus top. Note that as early as in 1983 the Spinhirne's research group[7] sounded thick cumulus from onboard a WB–57F aircraft flying at the altitude of 19 km. The published results are very interesting, however, they were not mathematically processed, and only presented in the form of 2D profiles of intensity and depolarization of the return signals.

The flights over ocean have been performed along complex routes, because they were intended for approbation of the airborne lidar sensing methods as the means for satellite underflight laser sounding. Figure 2 shows the navigation charts of two flights over ocean in the region of the Medvezhii Island in the Barents Sea. The flights were performed in two days. For them we have synchronous pictures taken from Nimbus–7 satellites.

Such a scheme of flights allowed us to survey a relatively large area (300 × 300 km in this case) of the cloud field and to save time and fuel. However, its main purpose was to obtain the information on the 2D distribution of the spatial structure of the cloud top. Under favorable conditions, namely, in the case of obtaining a continuous record of heights of a continuous cloud field with coordinate reference, we can correctly restore the fragment of the cloud field surface and estimate the statistical characteristics of the 2D distribution of the cloud top. Under less favorable conditions (presence of gaps in the continuous record of height values and/or presence of a multilevel field of broken clouds), it is possible to use standard 1D distributions, but containing the statistics on all the directions of the 2D space.

Of course, the IL–18DORR aircraft underwent a strong wind drift in the polar winds, so the actual flight trajectories differed from the regular geometrical figures (actual flight routes constructed from the data of the aircraft positioning system were given in Ref. 8). The cloud top heights at different areas of the cloud field for the flight on November 29, 1987, are given in the table in the right-hand part of the figure to avoid its complication. The data presented in the table is indicative of the presence of three to four cloud layers below the aircraft. The rms deviations of the cloud top heights in different areas of this cloud field varied from 15 to almost 150 m. The value of 315 m for the 9th area was obtained in the case when the laser beam illuminated lower cloud layers through breaks in the upper layer. In a similar experiment on November 27, 1987, we observed, as a rule, only one cloud layer. The mean heights of the cloud top at different places of the cloud field varied from 1600 to 1800 m. Only in the northern corner of this cloud square the mean height of the cloud top was 1970 m in one of the measurement files.

It should be noted that an IR radiometer was blind to changes in the cloud layers.

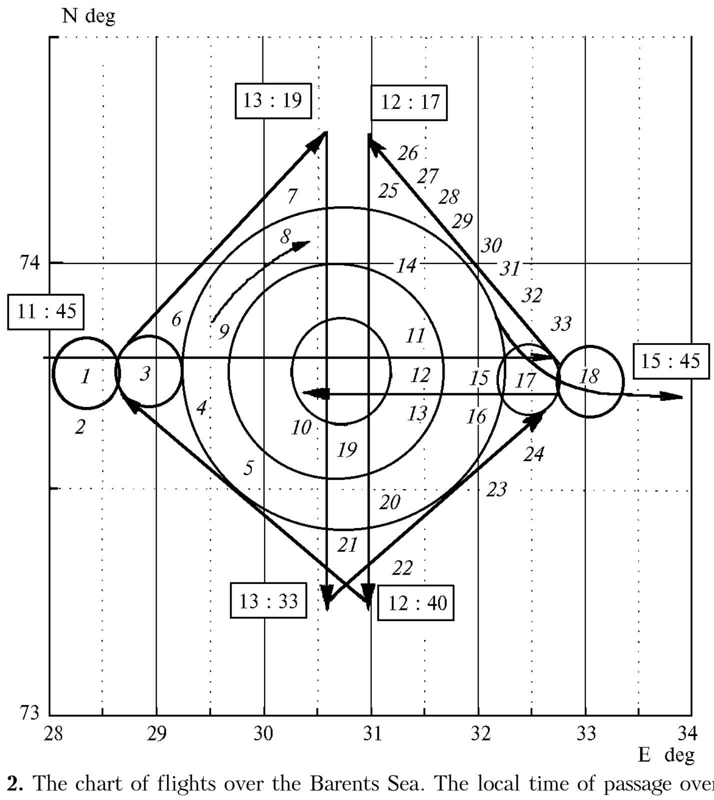

1 – (670 ± 21) m	
2 – (637 ± 25)	*18* – (814 ± 55) m
3 – (667 ± 21)	*19* – (1579 ± 151)
4 – (611 ± 16)	*20* – (1521 ± 104)
5 – (604 ± 22)	*21* – (1428 ± 129)
6 – (666 ± 86)	*22* – (1420 ± 113)
7 – (652 ± 15)	*23* – (968 ± 65)
8 – (820 ± 134)	*24* – (906 ± 61)
9 – (1856 ± 315)	*25* – (1214 ± 117)
10 – (950 ± 113)	*26* – (1485 ± 143)
11 – (638 ± 13)	*27* – (1500 ± 151)
12 – (950 ± 27)	*28* – (1268 ± 121)
13 – (881 ± 26)	*29* – (1297 ± 125)
14 – (687 ± 83)	*30* – (1368 ± 129)
15 – (675 ± 92)	*31* – (1412 ± 144)
16 – (865 ± 58)	*32* – (1415 ± 137)
17 – (964 ± 65)	*33* – (1399 ± 141)

Fig. 2. The chart of flights over the Barents Sea. The local time of passage over the key points on the route is shown in squares. Route sections are marked with italic numbers. The mean values and rms deviations of cloud top heights for these sections are given in the right-hand part of the figure. One degree of longitude corresponds to 30 km, and one degree of latitude corresponds to 111 km.

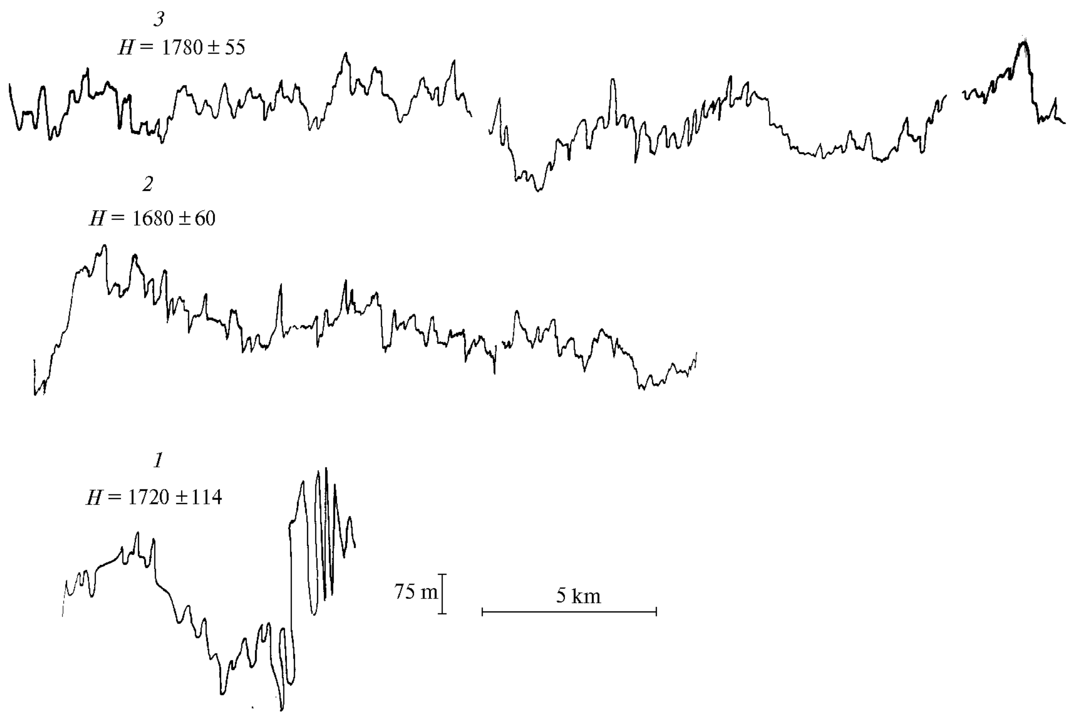

Fig. 3. Fragment of the measured cloud top profiles in the areas of the three concentric circles shown in Fig. 2 for the flight on November 27, 1987.

Figure 3 shows a fragment of the measured profiles of cloud top for the flight on November 27, 1987. Curves *1*, *2*, and *3* correspond to the three symmetric route rings (see Fig. 2) with the diameter about 15, 35, and 60 km. In this case both trends and gaps were present in the measurement files.

From here on we use the date of the experiment to mark the obtained results (files). Cloud type and cloud amount were determined by eye from aboard the aircraft, as well as by the maps of synoptic weather and pictures taken from space. Thus, we were able to determine not only the cloud type, but also the character of the dynamical state and conditional stage of evolution of a given cloud field. In such a way we have determined that the experiment on November 27, 1987, was conducted on the periphery of the central part of a frontal cloud belt coming from a developing Arctic cyclone. On November 29, 1987, this cyclone was at the stage of filling up, that is, the cloudiness began to dissipate. The sounding area was in the rear part of the cyclone, in which a cloud vortex was formed. Such conditions, especially over a water surface, are favorable for the development of convection. This is indicated by the presence of cumulus among broken stratus.

Estimation of the spectral density $Sp_h(f)$, which describes the frequency portrait of the process, plays an important part in analysis of the process dynamics. We describe the process of fluctuations of the cloud top height obtained from the data of laser sounding in terms of the spatial wavelengths λ of the cloud motions, and the spectral density, correspondingly, is determined by the spatial wave numbers $k = 2\pi/\lambda$. Estimation of the spectral density is based on the finite Fourier transform of the initial stationary random process $\{h_n(\lambda)\}$ defined on a finite interval $[\lambda_0 < \lambda < L]$. Here $\lambda_0 = 2\Delta l$ is the minimum spatial wavelength determined by the spatial resolution in a realization; $L = N\Delta l$ is the maximum wavelength limited by the finite number N of the sample size in a realization. The Fourier coefficients are calculated by the algorithm of the fast Fourier transform (FFT) thus determining the number of analyzed ordinates as a power of the base 2, so that always $N = 2^p$ (Ref. 6). To suppress leakage through side maxima, the Hann time window was used. For obtaining a stable spectral estimate and smoothing its values, calculation by overlapping sections is used, in which the initial realization is divided into a set of 50-% overlapping subintegrals. The error of estimation of the spectral density ε calculated in such a way is equal to $1/\sqrt{n_d}$ and for all experiments in the case of dividing into $n_d \cong N/100$ intervals was, on the average, 10 to 20%.

Let us consider the structure of the cloud top fluctuations for the case of sounding of marine clouds by the scheme shown in Fig. 2. Figures 4 and 5 show the estimates of the spectral density of the cloud top height fluctuations over the set of realizations $\{h_n\}$ obtained from sounding of cloud formations on November 27 and 29, 1987 (although the cloud formations were the same in both of the experiments, they were at different stages of evolution). On the whole, these figures characterize the dynamic state and the spatial structure of the cloud field. Thus, for the stratus field being at the stage of development (as was noted above) on November 27 we have the power spectrum shown in Fig. 4. It is very close to the classical "−5/3B power law. We can state that it holds in the inertial interval of the spatial wavelengths $0.04 < \lambda < 10$ km. In spite of some spread in values, they well fit the approximating straight line.

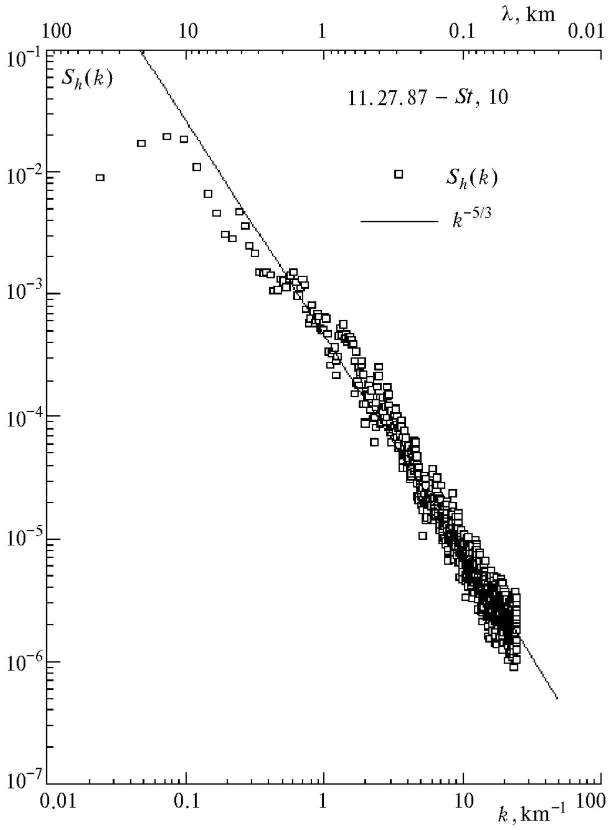

Fig. 4. Spectrum of the cloud top height fluctuations for developing *St* clouds over the ocean.

Figure 5 presents data collected on November 29, 1987, i.e., the second day of sounding. In this day the cloud amount was 8, rather than 10, as in the previous case. Besides, on November 29 we observed stratocumulus characterized by the beginning of the cloud field decomposition. In this case the "−5/3B law has more narrow domain of applicability. From below it is limited by the bend at the wavelength about 100 m, after which the fluctuations decrease faster. This bend is caused by physical destruction of cloud elements of the decomposing cloud field. From above it is limited by the pronounced outer scale (λ about 2 to 4 km) of repetition of the spatial structure of convective-type clouds, which were present in the cloud field.

Note that the $S_h(k)$ spectrum as a whole is less smooth in this case. Our estimates of the error in calculation of $S_h(k)$ show that local peaks and dips in this case are significant. Consequently, they are indicative of the presence of some periodic components in the structure of the cloud top.

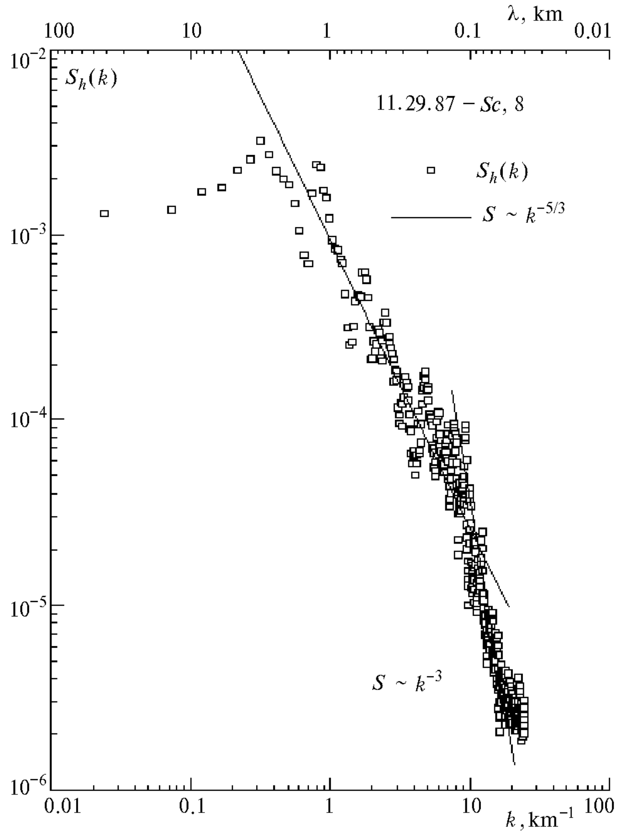

Fig. 5. Spectrum of the cloud top height fluctuations for decomposing oceanic *Sc* clouds.

Thus, clear difference in the behavior of the analyzed components allow the conclusion to be drawn that this sounding technique can be used for diagnostics of different cloud fields. This is very useful from the viewpoint of conducting underflight lidar experiments in support of space-based observations.

References

1. S.Yu. Popov and G.A. Titov, Atmos. Oceanic Opt. **7**, No. 3, 154–157 (1994).
2. A.I. Abramochkin, V.V. Zanin, I.E. Penner, A.A. Tikhomirov, and V.S. Shamanaev, Opt. Atm. **1**, No. 2, 92–96 (1988).
3. L.T. Matveev, *Course of General Meteorology. Atmospheric Physics* (Gidrometeoizdat, Leningrad, 1976).
4. V.S. Shamanaev, Atmos. Oceanic Opt. **5**, No. 7, 444–447 (1992).
5. I.E. Penner, I.V. Samokhvalov, V.S. Shamanaev, and I.A. Shnaider, in: *Abstracts of Reports at the Ninth All-Union Symposium on Laser and Acoustic Sounding of the Atmosphere* (Tomsk, 1987), Part 1, pp. 212–216.
6. J.S. Bendat and A.G. Piersol, *Random Data: Analysis and Measurement Procedures* (Willey, New York, 1971).
7. J.D. Spinhirne, M.Z. Hansen, and J. Simpson, J. of Climate and Applied Meteorology **22**, No. 8, 1319–1331 (1983).
8. I.E. Penner and V.S. Shamanaev, in: *Abstracts of Reports at the Tenth All-Union Symposium on Laser and Acoustic Sounding of the Atmosphere* (Tomsk, 1989), Part 1, pp. 139–143.